This article was downloaded by: [University of California, San Diego]
On: 09 August 2012, At: 14:14
Publisher: Taylor & Francis
Informa Ltd Registered in England and Wales Registered Number: 1072954
Registered office: Mortimer House, 37-41 Mortimer Street, London W1T 3JH, UK

Molecular Crystals and Liquid Crystals

Publication details, including instructions for authors and subscription information:
http://www.tandfonline.com/loi/gmcl20

Structure of Supramolecular Polymers Generated via Self-Assembly through Hydrogen Bonds

D. Sarazin [a], M. Schmutz [a], J.-M. Guenet [a], A. Petitjean [b] & J. M. Lehn [b]

[a] Institut Charles Sadron (ICS), Strasbourg, Cedex, France

[b] Institut de Science et d'Ingénierie Supramoléculaires (ISIS), Strasbourg, Cedex, France

Version of record first published: 22 Sep 2010

To cite this article: D. Sarazin, M. Schmutz, J.-M. Guenet, A. Petitjean & J. M. Lehn (2007): Structure of Supramolecular Polymers Generated via Self-Assembly through Hydrogen Bonds, Molecular Crystals and Liquid Crystals, 468:1, 187/[539]-201/[553]

To link to this article: http://dx.doi.org/10.1080/15421400701229990

PLEASE SCROLL DOWN FOR ARTICLE

Full terms and conditions of use: http://www.tandfonline.com/page/terms-and-conditions

This article may be used for research, teaching, and private study purposes. Any substantial or systematic reproduction, redistribution, reselling, loan, sub-licensing, systematic supply, or distribution in any form to anyone is expressly forbidden.

The publisher does not give any warranty express or implied or make any representation that the contents will be complete or accurate or up to date. The accuracy of any instructions, formulae, and drug doses should be independently verified with primary sources. The publisher shall not be liable for any loss, actions, claims, proceedings, demand, or costs or damages whatsoever or howsoever caused arising directly or indirectly in connection with or arising out of the use of this material.

Downloaded by [University of California, San Diego] at 14:14 09 August 2012

Mol. Cryst. Liq. Cryst., Vol. 468, pp. 187/[539]–201/[553], 2007
Copyright © Taylor & Francis Group, LLC
ISSN: 1542-1406 print/1563-5287 online
DOI: 10.1080/15421400701229990

Taylor & Francis
Taylor & Francis Group

Structure of Supramolecular Polymers Generated via Self-Assembly through Hydrogen Bonds

D. Sarazin
M. Schmutz
J.-M. Guenet
Institut Charles Sadron (ICS), Strasbourg, Cedex, France

A. Petitjean
J. M. Lehn
Institut de Science et d'Ingénierie Supramoléculaires (ISIS), Strasbourg, Cedex, France

The molecular structure and the morphology of self-assembling systems through hydrogen-bonds between complementary molecules has been investigated by electron microscopy and scattering techniques (light and neutron). It is found that in solvents such as toluene one-dimensional filaments are chiefly produced while in solvents such as THF lateral aggregation also occurs.

Keywords: hydrogen-bonds; polymers; self-assembling systems

Downloaded by [University of California, San Diego] at 14:14 09 August 2012

INTRODUCTION

Self-assembly of small molecules has proven to be a valuable process for preparing large structures with a limited synthetic effort. Huge supermolecular species have been successfully prepared by taking advantage of the complementarity of recognition groups bases on hydrogen bonding [1], metal coordination [2] or donor-acceptor interactions [3]. These entities are often named *supramolecular polymers* due to their resemblence with classical covalent polymers.

The authors are grateful to Dr. Bruno DEME for experimental assistance on D11 camera at ILL.

Address correspondence to D. Sarazin, Institut Charles Sadron (ICS), UPR22 CNRS, BP40016, 4 rue Boussingault, Strasbourg, Cedex F-67083, France. E-mail: sarazin@ics.u-strasbg.fr, guenet@ics.u-strasbg.fr

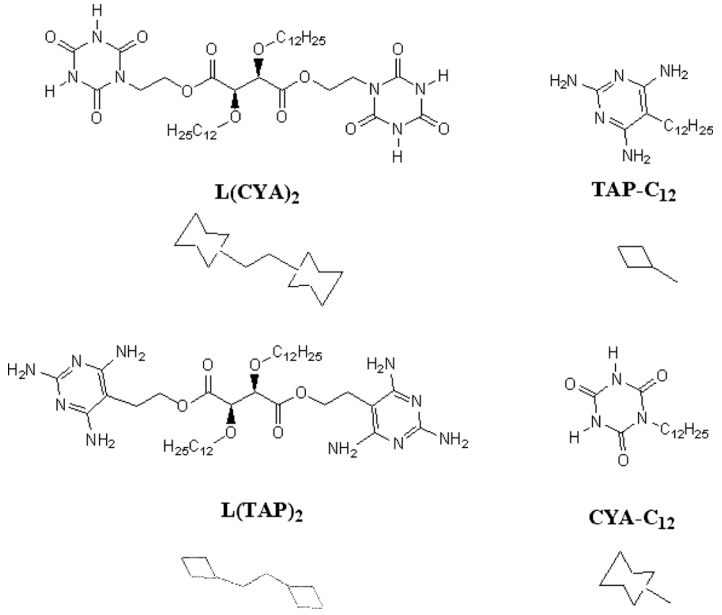

FIGURE 1 The two intercalates are shown with the so-called JANUS faces one called tri-oxocyanurate (CYA) bound at each ends of the L-tartric acid scaffold and on the right the triaminopyrimidineTAP-C_{12} bound on ancillary aliphatic chain.

Interestingly, these molecules self-assemble in organic solvents in rather dilute solutions, and thermoreversible gels, often designated as organogels, are formed in more concentrated solutions.

The cyanurate-based molecules portrayed in Figure 1 are liable to self-assemble through hydrogen bonding [1], as illustrated in Figure 2, and should therefore produce filaments that may or may not associate at later stages to produce larger threads.

The work presented in this article deals with structural investigations performed by electron microscopy and scattering techniques (neutron and light) intended for finding out whether these molecules do possess the propensity to form long filaments, and to what extent lateral aggregation competes with 1-D self-assembling. In particular, the role of the solvent is examined.

EXPERIMENTAL

Molecules

The self-assembling molecules used in this study are of two types: i) a dumbbell-like tartrate dicyanurate molecules, $L(CYA)_2$, with the

Downloaded by [University of California, San Diego] at 14:14 09 August 2012

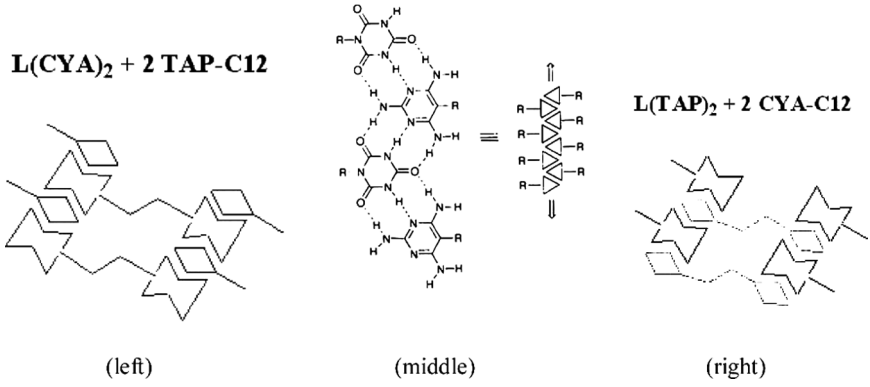

FIGURE 2 *left*: schematic assembly of $L(CYA)_2 + 2TAP - C_{12}$ to form JANUS-I; *right*: schematic assembly of $L(TAP)_2 + 2CYA - C_{12}$ to form JANUS-II. *middle*: the way hydrogen bonds are established between TAP-C_{12} and CYA-C_{12}.

triaminopyrimidine grafted with dodecane, TAP-C_{12} and ii) a dumb-bell-like tartrate triamino-pyrimidine, $L(TAP)_2$, with the cyanurate grafted with dodecane, CYA-C_{12} (see Fig. 1). The two "faces" TAP-C_{12} and CYA-C_{12} of these molecules are the keys of the self-assembling process, hence the designation of these systems as **JANUS**, the two-faced god in Roman mythology. In Figure 2 left is sketched the so-called **JANUS-I** which is a 50:50 mixture of both complementary molecules $L(CYA)_2 + TAP\text{-}C_{12}$. In Figure 2 right is sketched the so-called **JANUS-II** which is a 50:50 mixture of both complementary molecules $L(TAP)_2 + CYA\text{-}C_{12}$. Note that the length of a unit structure shown in Figures 2 and 3 is about 4–5 nm.

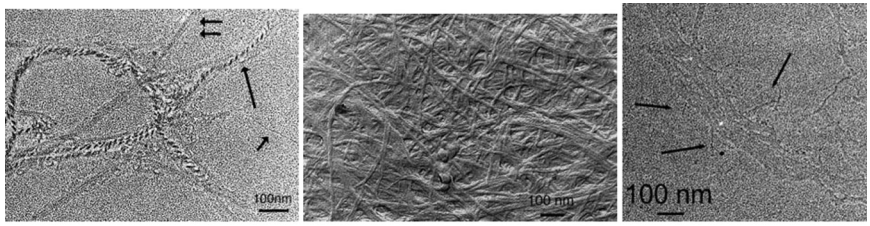

FIGURE 3 a) JANUS-II in dilute toluene solutions. The arrows point to the different kinds of structures. Long *1D-filaments* which associate to form ribbons as well as twisted ribbons; b) JANUS-II in a gel formed in toluene only twisted fibrils are observed with a cross-section diameter of 15 nm; c) JANUS-I in dilute toluene solutions. Long flat ribbons are observed. The latter are formed by lateral association of small fibrils seen on the ribbons side (arrows).

Downloaded by [University of California, San Diego] at 14:14 09 August 2012

Samples have been prepared in THF and in toluene at various concentrations typically ranging between 1×10^{-2} to 2×10^{-2} g/cm^3. Dissolving the systems is achieved by dispersion in the solvent under gentle stirring, and allowing the solutions to reach equilibrium for a minimum of 24 hrs.

Static Light Scattering

The laser light scattering is the common technique [4] which gives access to the shape of polymers through the mean square radius of gyration $\langle R_G \rangle_z$ and the particle scattering factor *P(q)*. Both wide- and small-angle static light scattering experiments were carried out. The wide-angle scattering intensity was measured by a in-house apparatus [5] equipped with (i) a red He–Ne laser of wavelength $\lambda_0 = 632.8$ nm in vacuum, (ii) a discrete-angle goniometer acting within the range from 20° to 155°, (iii) a Hamamatsu type photomultiplier as detector, (iv) a photo-counting device, and (v) a toluene matching bath. The vertical polarization of the incident beam with respect to the scattering plane has been used. The analyzer, arranged between the measuring cell and the photomultiplier, could assume both the vertical and the horizontal orientations. The first position allows measurement of the isotropic I_{VV} scattering while the second was applied in the study of the depolarized I_{VH} scattering intensity [6]. The excess of scattered intensity:

$$I_{VV}(q) = I_{VV\,\text{solution}} - I_{VV\,\text{solvent}} \tag{1}$$

was measured as a function of scattering vector $q = 4\pi n/\lambda_0 \sin\theta/2$ with an accuracy of 1% (θ the scattering angle, n the solvent refractive index). The values of Raleigh excess scattering intensity $R(q)$ were obtained through calibration with a benzene standard.

The toluene refractive index and the average refractive index increments of the assembly have been calculated by means of the Gladstone and Dale relation [7]. In toluene, these parameters are equal to $n = 1.4961$ and $dn/dC = 0.053$ ml/g, respectively, while in tetrahydrofuran (THF) they are equal to $n = 1.4050$ and $dn/dC = 0.050$ ml/g, respectively.

Preparation of the samples for the light scattering experiments has been carried out in two steps. In a first step, each component has been dissolved separately in methanol. The methanol solutions have been filtered to remove dust particles, and then freezed-dried in order to recover each species. In the second and final step, the light scattering solutions have been prepared by mixing the complementary constituents in filtered toluene and/or filtered THF. All solutions have been aged for a minimum of 48 hrs prior to any measurements.

Downloaded by [University of California, San Diego] at 14:14 09 August 2012

Downloaded by [University of California, San Diego] at 14:14 09 August 2012

Small-Angle Neutron Scattering

The experiments were performed on D11 camera located at the Institut Laue-Langevin (Grenoble, France). A wavelength of $\lambda_m = 0.6\,\text{nm}$ was used with a wavelength distribution characterized by a full width at half maximum, $\Delta\lambda/\lambda_m$, of about 10%. Neutron detection and counting was achieved with a built-in two-dimensional sensitive detector composed of 64×64 cells (further details are available on request at ILL website http://www.ill.fr). By varying the sample-detector distance the available q-range was $0.1 < q\ (\text{nm}^{-1}) < 2.5$ where $q = (4\pi/\lambda)\ \sin\ (\theta/2)$, θ being the scattering angle.

Cell efficiency correction was achieved by using the incoherent scattering of hydrogenous *cis*-decalin. The normalized intensity scattered is then written as:

$$I_N(q) = \left[\frac{\dfrac{I_s(q)}{T_s\delta_s} - \dfrac{I_e(q)}{T_e\delta_e}}{\dfrac{I_{dec}(q)}{T_{dec}\delta_{dec}} - \dfrac{I_e(q)}{T_e\delta_e}}\right] \tag{2}$$

in which $I(q)$, δ and T are the intensity, the thickness and the transmission respectively, corresponding with the appropriate subscript to the sample (s), the liquid *cis*-decalin (dec) and to the empty cell (e).

In order to extract the coherent intensity scattered by the hydrogenous self-assembled molecules (supramolecular polymer) the coherent intensity scattered by the solvent and the incoherent intensity scattered by the self-assembled molecules have to be subtracted from the total scattered intensity (the solvents being deuterated their incoherent scattering can be neglected). Fazel *et al.* [8] have established an experimental relation which allows calculation of the incoherent scattering of the hydrogenous supramolecular polymer:

$$I_{\text{inc}} = 8.65\frac{N_H}{V_H} \tag{3}$$

in which N_H is the number of proton per monomer and V_H the molar volume of the repeat unit of the supramolecular polymer. The absolute coherent intensity scattered by the hydrogenous supramolecular polymer finally reads:

$$I_A(q) = \frac{1}{K}\left[I_N(q) - (1 - \varphi_{sp})I_D(q) - \varphi_{sp}8.65\frac{N_H}{V_H}\right] \tag{4}$$

in which $I_D(q)$ is the normalized intensity scattered by the deuterated solvent, φ_{sp} the supramolecular polymer fraction and K a calibration

constant which reads:

$$K = \frac{4\pi(a_{sp} - ya_s)^2 \delta_{dec} T_{dec} N_A}{g(\lambda_m)(1 - T_{dec}) m_i^2} \quad (5)$$

in which a_{sp} is the coherent scattering amplitude of the supramolecular polymer, a_s the coherent scattering amplitude of the solvent, $y = V_{sp}/V_s$ i.e., the ratio of the molar volume of the supramolecular polymer ($V_{sp} = 1496\,\text{cm}^3/\text{mole}$) and of the solvent, δ_{dec} and T_{dec} the thickness and the transmission of the calibration sample, m_i the molecular weight of the repeat unit of the supramolecular polymer, and $g(\lambda_m)$ a constant which is camera-dependent and was measured by using Cotton's method [9].

Samples were prepared directly in quartz cells from HELLMA of optical paths of 2 and 5 mm. Deuterated toluene and deuterated THF were purchased from Aldrich and used without further purification.

Electron Microscopy

The samples were prepared as follows:

In the dilute regime, 5 μL drop were deposited onto a carbon coated grid and after 1 min adsorption the excess of liquid was removed with filter paper. Finally, the grid was rotary shadowed with PT/W at a 15° angle.

Gels cannot be prepared in this way but a replica was prepared after freeze fracturing instead. This technique preserves the internal structure of the gel. A small piece of the gel was placed between two copper holders and rapidly frozen in liquid nitrogen. The sandwiches were transferred into a home-made cryo-fracturing apparatus and the fracture was performed under high vacuum (10–7 torr) and then a thin layer of Pt/C (2 nm) was evaporated at a 45° angle. Finally, a reinforcing layer of carbon (20 nm) was evaporated at a 90° angle. The replicas were thoroughly washed with CHCl3 and picked up with bare 400 mesh grids.

The grids were observed in a CM12 microscope operating at 120 kV. SO163 Kodak films were used for imaging and were developed under standard condition.

RESULTS AND DISCUSSION

Morphology

The morphologies have been studied by electron microscopy. In Figure 3a is shown the morphology of JANUS-II after self-assembling in very dilute toluene solutions. Typically, three types of objects are

Downloaded by [University of California, San Diego] at 14:14 09 August 2012

observed. Small filaments with a cross-section diameter of about 4 nm (short arrow Fig. 3a), flat ribbons (short double arrow) and twisted ribbons (15 nm) (long arrow). The size of the cross-section diameter of the small filaments correspond approximately to what is expected with one, and only one arrangement as described in Figure 2. It is likely that ribbons made up of this arrangement have two stable structures: flat and twisted ribbons. In Figure 3b is shown the morphology of a gel in toluene obtained after freeze-fracturing process. Mainly twisted filaments (of cross-section diameter 15 nm) are observed. The morphology of JANUS-I in toluene is shown in Figure 3c. As with JANUS-II the basic structure is a filament (of cross-section diameter 4.5 nm) (as indicated by arrow), with a tendency to aggregate in flat ribbons. Inside the ribbons faint striations can be seen at glancing angle. These striations correspond to the individual filaments. Figure 4 shows the morphology of Janus II in THF. Long rigid ribbons together with platelets of about the same cross-section are observed.

Downloaded by [University of California, San Diego] at 14:14 09 August 2012

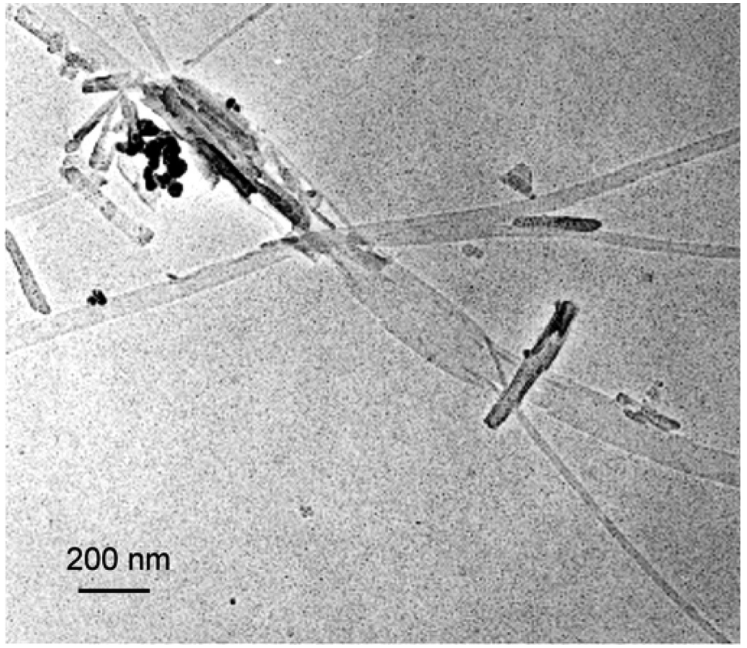

FIGURE 4 JANUS-II as obtained from dilute THF solutions. Two kind of structures are observed. Long flat ribbons with a very high persistence length and crystalline platelets.

Neutron Scattering

JANUS-I has been investigated in toluene and THF while JANUS-II has only been studied in toluene. As electron microscopy has revealed objects with high aspect ratio, we shall use in what follows theoretical expressions dealing with such structures of the type [10]:

$$I(q) \propto \frac{\pi \mu_L}{q} \times \varphi(q\sigma) \tag{6}$$

where μ_L is the mass per unit length in g/mol × nm, $\varphi(q\sigma)$ is a function related to the cross-section of the objects, wherein σ is a characteristic length.

In toluene JANUS-I produces different molecular structures depending upon its concentration. For a concentration $C_{J\text{-}I} = 0.0126\,\mathrm{g/cm^3}$, the scattering curve displayed in Figure 5 can be fitted by the following equation [10] for $q > 0.1\,\mathrm{nm^{-1}}$:

$$q^2 I(q) \propto \pi \mu_L C_{J-I} \times \frac{4J_1^2(qr)}{q^2 r^2} \times \left[\pi q - \frac{2}{\langle L \rangle}\right] \tag{7}$$

which corresponds to the scattering by filaments of cross-section radius r, mass per unit length μ_L and average length $\langle L \rangle$ in the range $q\langle L \rangle > 1$, and where J_1 is the Bessel function of 1st kind and 1st order. Here, it is found $r = 2 \pm 0.2\,\mathrm{nm}$. This value is in good agreement with the findings from electron microscopy. Determination of

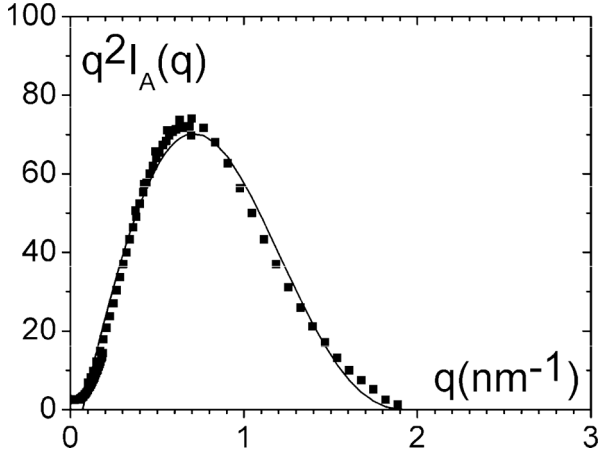

FIGURE 5 Neutron scattering data in absolute units plotted by means of a Kratky-plot ($q^2 I_A(q)$ vs q). JANUS-I/toluene $C_{J-I} = 1.26 \times 10^{-3}\,\mathrm{g/cm^3}$. The solid line corresponds to the best fit (see text for details).

Downloaded by [University of California, San Diego] at 14:14 09 August 2012

the mass per unit length thanks to absolute calibration yields $\mu_L = 2140\,\mathrm{g/mol} \times \mathrm{nm}$. The cross-section radius together with the mass per unit length are indicative of self-assembled structures where there is only one basic repeat unit as sketched in Figure 2 in the cross-section diameter. We shall therefore designate this structure as *1-D filaments* in what follows.

Note that the fit is strictly valid for twisted ribbons that scatter like solid cylinder provided that $qP < 2\pi$ where P is the pitch of the twist. In the case of a flat ribbon of length L_c, width l_c and thickness δ_c the form factor has been derived by Mittelbach and Porod [11] for $L_c >> l_c$ and $l_c > \delta_c$:

$$q^2 I(q) \approx \frac{\pi q}{L_c} \times \frac{2}{\pi} \int_o^{\pi/2} \left[\frac{\sin q l_c/2 \cos\theta}{q l_c/2 \cos\theta} \times \frac{\sin q\delta_c/2 \sin\theta}{q\delta_c/2 \sin\theta} \right]^2 \sin\theta\, d\theta \qquad (8)$$

This gives for $qL_c>$ and $ql_c > 1$ with $q\delta_c < 1$:

$$q^2 I(q) \approx 2\pi\mu_S \times \exp -q^2\delta_c^2/12 \qquad (9)$$

in which μ_S is the mass per unit area.

We note that for $q < 0.1\,\mathrm{nm}^{-1}$ a $1/q^2$ behaviour is seen which may suggests the presence of a certain amount of flat ribbons of thickness smaller than 0.5 nm (approximate thickness of the system $L(CYA)_2$+ 2TAP-C12) as the exponential corrective term in relation 8 is very close to 1. This is in agreement with the electron microscopy observations that have revealed the presence of flat ribbons. Yet, light scattering results presented below rather suggest large amounts of twisted ribbons.

The fact that one can measure an average length $\langle L \rangle \approx 9\,\mathrm{nm}$ for the filaments indicate the existence of short, straight filaments although very long filaments are also present. That the average length corresponds to the first moment of the length distribution (number average) enhances the effect due to the shortest filaments.

By increasing the concentration of JANUS-I in toluene ($C_{J-I} = 18.6 \times 10^{-2}\,\mathrm{g/cm^3}$), the scattering curve is altered (Fig. 6). Only one radius is not sufficient for fitting the curve, which implies the occurrence of sideways aggregation of the original filaments. One has to use the following equation instead:

$$q^2 I(q) \propto \pi^2 d_f C_{J-I} \times \sum_1^n X_n (r/n)^2 \times \frac{4J_1^2(qr/n)}{q^2(r/n)^2} + Cte \qquad (10)$$

Downloaded by [University of California, San Diego] at 14:14 09 August 2012

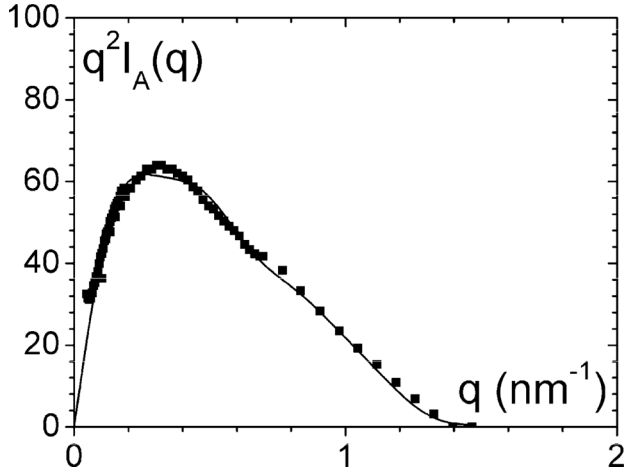

FIGURE 6 Neutron scattering data in absolute units plotted by means of a Kratky-plot ($q^2I_A(q)$ vs q). JANUS-I/toluene $C_{J-I} = 18.6 \times 10^{-3}$ g/cm^3. The solid line corresponds to the best fit (see text for details).

where X_n is the fraction of species of cross-section radius r/n, with $\sum_1^n X_n = 1$, d_f is the density in g/cm^3 of the threads since $\mu_L = \pi r^2 d_f$. Here the constant takes into account possible random, lateral aggregation. In the present case the best fit was achieved with:

$$q^2 I(q) \propto \pi^2 d_f C_{J-I} \times \left[X_1 r^2 \times \frac{4J_1^2(qr)}{q^2(r)^2} + X_2(r/2)^2 \times \frac{4J_1^2(qr/2)}{q^2(r/2)^2} + X_4(r/4)^2 \times \frac{4J_1^2(qr/4)}{q^2(r/4)^2} \right] + Cte \qquad (11)$$

where $r = 10.2$ nm, and correspondingly $r/2 = 5.1$ nm, $r/4 = 2.55$ nm, and with $X_1 + X_2 + X_4 = 1$.

These Figures mean that original 1-D filaments are still present ($r = 2.55$ nm) but threads are produced by aggregation of up to about 16 filaments by estimating the aggregation number through the square ratio of the largest radius with respect to the original filament radius.

The situation is at variance in JANUS-I/THF solutions. For a concentration quite close to the most dilute solutions used with toluene, namely 0.011 g/cm^3, the scattering curve represented in Figure 7

Downloaded by [University of California, San Diego] at 14:14 09 August 2012

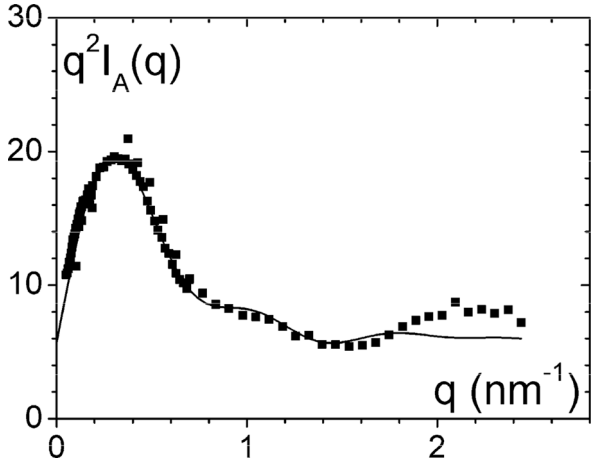

FIGURE 7 Neutron scattering data in absolute units plotted by means of a Kratky-plot ($q^2 I_A(q)$ vs q). JANUS-II/toluene $C_{J-II} = 0.55 \times 10^{-3}\,\mathrm{g/cm^3}$. The solid line corresponds to the best fit (see text for details).

differs quite dramatically from that in toluene. This scattering curve can be fitted with the following equation:

$$q^2 I(q) \propto \pi^2 d_f C_{J-I} \times \left[X_1 r^2 \times \frac{4J_1^2(qr)}{q^2(r)^2} + X_2 (r/2)^2 \times \frac{4J_1^2(qr/2)}{q^2(r/2)^2} + X_3 (r/3)^2 \times \frac{4J_1^2(qr/3)}{q^2(r/3)^2} \right] + Cte \qquad (12)$$

wherein $r = 23.5\,\mathrm{nm}$, and correspondingly $r/2 = 11.8\,\mathrm{nm}$, $r/3 = 7.8\,\mathrm{nm}$ and again with $X_1 + X_2 + X_3 = 1$.

This theoretical fit is in agreement with the observations made by electron microscopy and therefore indicates that original filaments as were observed in toluene no longer exist in THF. THF therefore promotes strong sideways aggregation. This means in particular that the largest threads consist of about hundred side-ways bunched *1-D filaments* while the smallest threads contain about ten *1-D filaments*.

JANUS-II has only been studied in toluene. The scattering curve obtained for a concentration $C_{J-II} = 0.55 \times 10^{-3}\,\mathrm{g/cm^3}$ is shown in Figure 8. A satisfactory fit can be obtained by means of the following equation where n values are no longer integer:

Downloaded by [University of California, San Diego] at 14:14 09 August 2012

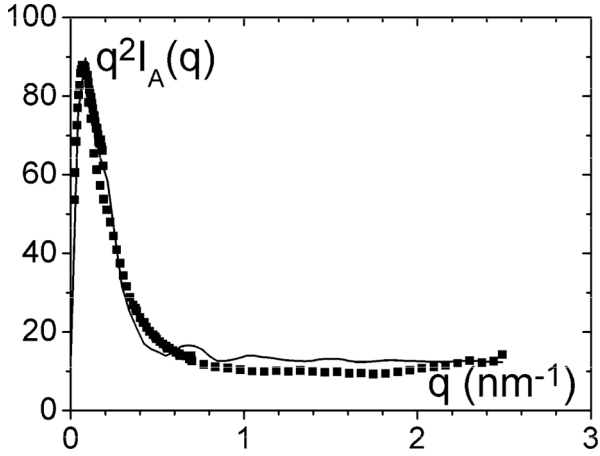

FIGURE 8 Neutron scattering data in absolute units plotted by means of a Kratky-plot ($q^2 I_A(q)$ vs q). JANUS-I/THF $C_{J-I} = 11 \times 10^{-3}$ g/cm^3. The solid line corresponds to the best fit (see text for details).

$$q^2 I(q) \propto \pi^2 d_f C_{J-II} \times \left[X_1 r^2 \times \frac{4J_1^2(qr)}{q^2(r)^2} + X_2 (r/2.63)^2 \times \frac{4J_1^2(qr/2.63)}{q^2(r/2.63)^2} \right] + Cte \tag{13}$$

wherein $r = 4.86$ nm, and correspondingly $r/2.63 = 1.84$ nm.

Here again, the 1-D filaments exist on their own ($r = 1.84$ nm) but sideways aggregation also occurs and produces threads made up with about seven 1-D filaments.

Light Scattering

In Figure 9 is shown a typical Zimm-plot obtained for JANUS-I in toluene in a concentration range from 5.7×10^{-4} g/cm^3 down to 1.23×10^{-4} g/cm^3, namely in a very dilute state. This Zimm-plot allows one to determine easily the weight-average molecular weight M_w and a z-average radius of gyration $\langle R_G \rangle_z$. It is found $M_w = 1.1 \times 10^7$ g/mole and $\langle R_G \rangle_z = 229 \pm 30$ nm.

In the case of straight, high aspect ratio objects, the radius of gyration is simply expressed through [12]:

$$R_G^2 = \frac{L^2}{12} \tag{14}$$

where L is the length of the ribbon.

Downloaded by [University of California, San Diego] at 14:14 09 August 2012

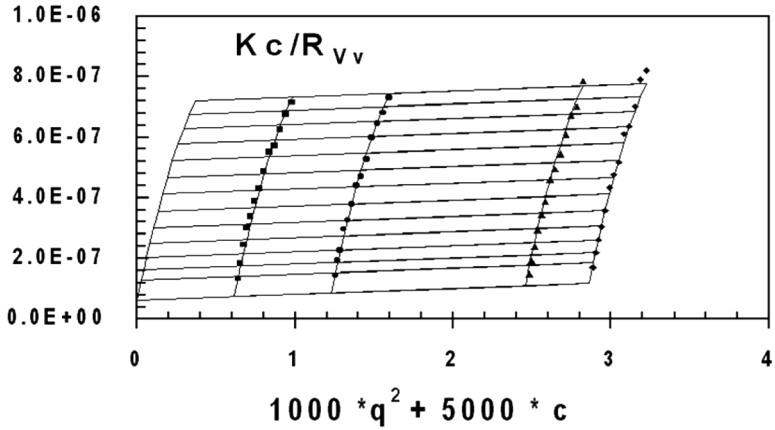

FIGURE 9 Normalized Zimm-plot for JANUS-I/Toluene solutions measured at $T = 35°C$ for different self assembly concentrations (◆) 5.718×10^{-4} g/cm^3, (▲) 4.908×10^{-4} g/cm^3, (●) 2.454×10^{-4} g/cm^3, (■) 1.227×10^{-4} g/cm^3.

The molar mass of one repeat unit in the case of JANUS-I is $M_{JANUS-1} = 1354$ g/mole, which means that for the above value of the weight-average molecular weight there are about 8120 repeat units in the scattering objects. If the object had all a flat, straight ribbon conformation, and taking into account that the "height" of the repeat unit is about 0.5 nm, one would expect a radius of gyration of about $\langle R_G \rangle_w \approx 1200$ nm. In view of the experimental radius of gyration $\langle R_G \rangle_z = 229 \pm 30$ nm this therefore implies that the stablest conformation in solution is most probably the twisted ribbon. The length of the structure has to be reduced by about 5 times for matching the experimental radius of gyration. If one considers a cross-section radius r of about 2 nm for these twisted ribbons, this should imply a pitch of $p = 2.6$ nm since the reduced length L_r is related to the extended ribbon length L through:

$$L_r = \frac{Lp}{\sqrt{p^2 + 4\pi^2 r^2}} \tag{15}$$

This figure ($p = 2.6$ nm) is consistent with electron microscopy observations whenever twisted ribbons are seen. Yet, it should be stressed that the figure of 2.6 nm is only indicative since the twisted ribbons display some flexibility, as is discussed below, and also that the experimental radius of gyration is the z-average value while the molecular weight is the weight-average value. Taking into account flexibility would decrease the value of pitch while polydispersity in supramolecular polymer length would increase it.

Downloaded by [University of California, San Diego] at 14:14 09 August 2012

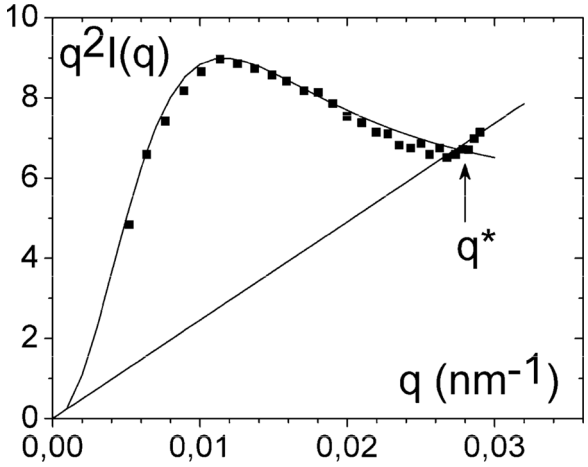

FIGURE 10 Normalized light scattering data plotted by means of a Kratky-plot ($q^2 I_A(q)$ vs q). JANUS-II/THF at T = 35°C with $C_{J-II} = 0.36 \times 10^{-3}$ g/cm^3. The solid line is a best fit with relation 16. The straight line stands for a rod-like behaviour.

When concentration is increased the condition $qR_G < 1$ is no longer fulfilled. The light scattering experiments correspond then to the so-called intermediate range. As can be seen in Figure 10 a Kratky-plot ($q^2 I(q)$ vs q representation) shows a conspicuous hump. This points to random aggregation of filaments with one another. This means that sideways aggregation between two filaments occurs randomly over a limited length. This implies that the filaments possess a certain degree of flexibility otherwise long straight fibrils would be obtained whose scattering would totally differ. Clearly, these filaments are straight over the range of distances probed by neutron scattering (typically <100 nm) but flexible at distances probed by light scattering (over 100 nm). A fit can be achieved with a relation derived by Guenet and Picot [13]:

$$I(q) = \frac{P_o(q)}{N_c^2} \times \left[\frac{2P_o^{N_c+1}(q) - N_c P_o^2(q) - 2P_o(q) + N_c}{[1 - P_o(q)]^2} \right] \tag{16}$$

where $P_o(q)$ is the form factor of one filament and N_c is the number of filaments in the aggregates. Contemplating flexible filaments, a gaussian function can be used for $P_o(q)$ [4]:

$$P_o(q) = \frac{2}{q^4 R^4} [\exp -q^2 R^2 + q^2 R^2 - 1] \tag{17}$$

Downloaded by [University of California, San Diego] at 14:14 09 August 2012

The fit gives $N_c = 9$ with $R = 110\,\text{nm}$. The relatively small radius of gyration (110 nm) indicates that branching occurs in THF for filaments shorter than in toluene. At larger q, a rod-like behaviour seems to be seen. The filament flexibility is again consistent with the electron microscopy findings.

CONCLUDING REMARKS

The set of experiments presented in this article confirm that molecules of the JANUS type as described here tend to form 1-D filaments through self-assembling process. The 1-D filament state is obtained at low dilutions and in non-polar solvents such as toluene. Conversely, in more polar solvents such as THF sideways aggregation occurs, and correspondingly branching. This is possibly due to the aliphatic substituents in C_{12} which are exposed to the solvent molecules. These substituents interact better with toluene than with THF, preventing in the former further sideways aggregation while promoting it in the latter.

Although electron microscopy is considered a destructive technique due to the special preparation undergone by the sample, the conclusions drawn from this technique proved to be in very good agreement with those drawn from neutron scattering, a non-destructive technique.

REFERENCES

[1] Lehn, J. M. (1995). *Supramolecular Chemistry: Concepts and Perspectives*, VCH-Weinheim, New York.
[2] Dammer, C., Terech, P., Maldivi, P., & Guenet, J. M. (1995). *Langmuir*, *11*, 1500.
[3] Berl, V., Schmutz, M., Krische, M. J., Khoury, R. G., & Lehn, J. M. (2002). *Chemistry-A European Journal*, *8*, 1227.
[4] Debye, P. (1947). *Phys. Coll. Chem.*, *51*, 18.
[5] Libeyre, A., Sarazin, D., & François, J. (1981). *J. Polym. Bull.*, *4*, 53.
[6] Chu, B. (1991). *Laser Light Scattering*, 2nd ed., Academic Press: London.
[7] Gladstone, J. & Dale, H. (1863). *Phil. Trans.*, *153*, 317.
[8] Fazel, N., Brûlet, A., & Guenet, J. M. (1994). *Macromolecules*, *27*, 3836.
[9] Cotton, J. P. (1991). In: *Neutron, X-ray and Light Scattering*, Lindner, P. & Zemb, T. (Eds.), Elsevier.
[10] (a) Fournet, G. (1951). *Bull. Soc. Franç. Minèr. Crist.*, *74*, 39.
(b) Oster, G. & Riley, D. P. (1952). *Acta Cryst.*, *5*, 272.
(c) Pringle, O. A. & Schmidt, P. W. (1971). *J. Appl. Cristallogr.*, *4*, 290.
[11] Mittelbach, P. & Porod, G. (1961). *Acta Phys. Austriaca*, *14*, 405.
[12] Guenet, J. M. (1980). *Macromolecules*, *13*, 387.
[13] Guenet, J. M. & Picot, C. (1981). *Macromolecules*, *14*, 309.

Downloaded by [University of California, San Diego] at 14:14 09 August 2012